UPPSALA
UNIVERSITET

Digital Comprehensive Summaries of Uppsala Dissertations from the Faculty of Science and Technology 1153

Kinematics and Internal Deformation of Granular Slopes

ZHINA LIU

ACTA
UNIVERSITATIS
UPSALIENSIS
UPPSALA
2014

ISSN 1651-6214
ISBN 978-91-554-8968-7
urn:nbn:se:uu:diva-223792

Dissertation presented at Uppsala University to be publicly examined in Hambergsalen, Geocentrum, Villavägen 16, Uppsala, Friday, 13 June 2014 at 10:00 for the degree of Doctor of Philosophy. The examination will be conducted in English. Faculty examiner: Professor Dominique Frizon de Lamotte (Université de Cergy-Pontoise, Département Géosciences et Environnement).

Abstract
Liu, Z. 2014. Kinematics and Internal Deformation of Granular Slopes. *Digital Comprehensive Summaries of Uppsala Dissertations from the Faculty of Science and Technology* 1153. 39 pp. Uppsala: Acta Universitatis Upsaliensis. ISBN 978-91-554-8968-7.

Flow-like mass movement is the most destructive landslide and causes loss of lives and substantial property damage throughout the world every year. This thesis focuses on the spatial and temporal changes of the mass movement in terms of velocity and displacement within the failure mass, and the spatial and temporal distribution of the three dimensional internal deformation of the granular slopes using discrete element method, physical experiments, and natural landslides. We have also studied the effect of weak horizons on the kinematics and internal deformation of granular slopes. Numerical model results show the following features related to a failure mass. The failure mass flows downwards in an undulating pattern with a distinctive velocity heterogeneity. Dilatation within the failure mass is strongly dependent on its mechanical properties. A larger mass moves downslope and the mass moves faster and further in the model with lower internal friction and cohesion. The presence of weak horizons within the granular slope strongly influences displacement, location of the failure surface, and the amount of the failure mass. In addition, results from analogue models and natural landslides are used to outline the mode of granular failure. The collapse of granular slopes results in different-generation extensional faults in the back of the slope, and contractional structures (overturned folds, sheath folds and thrusts) in the toe of the slope. The first-generation normal faults with a steep dip (about 60º) cut across the entire stratigraphy of the slope, whereas the later-generation normal faults with a gentle dip (about 40º) cut across the shallow units. The nature of the runout base has a significant influence on the runout distance, topography and internal deformation of a granular slope. Good agreements are found between models and nature for the collapse of granular slopes in terms of the similar structural distribution in the head and toe of the failure mass and different generations of failure surfaces. The presence of a weak horizon within the granular slope has a significant influence on the granular failure and three dimensional internal deformation of the failure mass.

Keywords: granular flow, kinematics, internal deformation, particle flow method, analogue modeling, natural landslides

Zhina Liu, Department of Earth Sciences, Villav. 16, Uppsala University, SE-75236 Uppsala, Sweden.

ISSN 1651-6214
ISBN 978-91-554-8968-7
urn:nbn:se:uu:diva-223792 (http://urn.kb.se/resolve?urn=urn:nbn:se:uu:diva-223792)

To my family

List of Papers

This thesis is based on the following papers, which are referred to in the text by their Roman numerals.

I **Liu, Z.** and Koyi, H.A. (2013) Kinematics and internal deformation of granular slopes: insights form discrete element modeling. *Landslides*, 10: 139-160.

II **Liu, Z.** and Koyi, H.A. (2013) The impact of a weak horizon on kinematics and internal deformation of a failure mass using discrete element modeling. *Tectonophysics*, 586: 95-111.

III **Liu, Z.**, Koyi, H.A., Swantesson, J.O.H., Nifouroushan, F. and Reshetyuk, Y. (2013) Kinematics and 3-D internal deformation of granular slopes: Analogue models and natural landslides. *Journal of Structural Geology*, 53: 27-42.

IV **Liu, Z.** and Koyi, H.A. (2014) Analogue modeling of the collapse of non-homogeneous granular slopes along weak horizons. *Tectonophysics, under review.*

Reprints were made with permission from the respective publishers.

In all the above listed papers under the supervision from Prof. Koyi, I ran numerical models, performed physical experiments, did field work, analyzed and interpreted model results, and wrote the manuscripts. For paper III, the other co-authors also contributed to field assistance and comments to the manuscript.

Contents

1 Introduction

1.1 Flow-like landslides

Varnes (1978) suggested that all slope movements involving significant internal distortion/deformation of a failure mass can be classed as flows. However, it is often difficult to distinguish whether internal deformation or boundary sliding is dominant during the downslope movement of the failure mass. Hence, landslides that display either internal deformation or boundary sliding are defined as flow-like landslides (Hutchinson, 1988). Hunger et al. (2001) and Hutchinson (2004) reviewed the classification of the flow-like landslides in granular materials, and summarized four groups of flow-like form landslides: debris flow, flow slides, rock avalanches and mudslides. A flow-like landslide often begins as a slide, forming and propagating a slip surface, but continues spreading outside the failure area and moving over a long distance (Hunger et al., 2001; Picarelli et al., 2008). Flow-like landslides are the most destructive among all types of landslides (Hunger, 2003). Those slope movements, which have long travel distance, high velocity and large volume of failure mass, are the most difficult to prevent and cause loss of lives and substantial property damage throughout the world every year (Hunger et al., 2001; Hutchinson, 2004). As such, it is of great significance to understand the kinematics and dynamics of the flow-like mass movement of granular materials.

Many researchers have been studying the problem of the flow-like mass movement, where most of the focus has been on the run-out distance analysis (Hansen, 1997; Hungr, 1995 and 2009; Miao et al., 2001; Valentino et al., 2008; Staron, 2008; Wang et al., 2010) and/or the triggering and motion mechanisms of flows (Hungr, 2003 and 2008; Picarelli et al., 2008; Li et al., 2012). The results of such studies show that the flow-like movement can be triggered by a mechanism of general shear failure, and commonly displays high internal deformation (Bromhead, 2000; Hungr et al., 2001; Picarelli et al., 2008). However, few investigations have been carried out on the kinematics and internal deformation of the flow-like landslides.

Some researchers investigated the kinematics and deformation of the ground surface of flow-like landslides using field monitoring techniques such as Global Positioning System techniques (GPS; Gili et al., 2000; Mora et al., 2003), Interferometry Synthetic Aperture Radar (InSAR; Peyret et al., 2008; Liu et al., 2011; Barla et al., 2010) and the terrestrial laser scanning

(TLS; Teza et al., 2007 and 2008; Oppikofer et al., 2009; Sturzenegger and Stead, 2009). They mainly measured and quantified the spatial and temporal evolution of the surface displacement of a landslide, computed velocity vector fields and a strain field on ground surface and thus characterized a landslide ground surface kinematics. For instance, Peyret et al. (2008) analyzed the surface displacement of Kahrod landslide in Iran by GPS and InSAR, and concluded that surface deformation is roughly homogeneous over the whole landslides and the time evolution of surface deformation does not exhibit significant changes. Liu et al. (2011) identified surface deformation at Badong in China from 2003 to 2010 by InSAR, and found a heterogeneity velocity vector fields on ground surface. Field monitoring is one of the most effective methods to investigate the mass movement of landslides; however, it is technically impossible to monitor the internal deformation of the failure mass at present using field monitoring techniques.

Other researchers investigated the movement and deformation of a failure mass within the flow-like landslides using numerical and/or physical modeling. Campbell et al. (1995) studied global deformation in large-scale landslides by a discrete particle computer simulation, and showed that the mass is shearing throughout the avalanche body instead of moving as a nearly solid block. Bui et al. (2008) studied the failure patterns of gravitational flow for both non-cohesive and cohesive soil by Lagrangian mesh-free particles method and physical experiments. Thompson et al. (2009) investigated the internal deformations during the process of large-scale volcanic debris avalanches using the particle flow method. Roy and Mandal (2009) used sand slope models with passive layers to recognize the propagation of slope failure in the sand bed due to overburden loading. They found that the process involves both compaction and shear failure, and the shear failure propagates fast in the slope direction and destabilizes the slope. Chen et al. (2011) investigated the movement of dry granular soil slopes, and concluded that the slope angle and the internal friction angle of soil influence the front velocity significantly. Lajeunesse et al. (2005), Siavoshi and Kudrolli (2005), and Lube et al. (2005 and 2007) performed laboratory experiments to simulate the collapse of granular slopes. They concluded that the area/volume of static material grows with time and the interface separating static and flowing regions propagates towards the free surface with time. These researchers provided some limited understanding about the deformation pattern within the failure mass after mass movement of granular slopes, but the internal deformation of the flow-like movement still remains poorly understood.

1.2 The impact of weak horizons

It is well known that the slope stability is strongly related to the geometry and mechanical properties of any pre-existing discontinuity (Naghadehi et

al., 2011; Bois et al., 2012; Saintot et al., 2011). An open discontinuity (e.g., joint, fault, or bedding plane) filled with soft filling material such as clay gouge, which can be called a weak horizon, has much lower shear strength than the surrounding slope material. In addition, in many sedimentary rocks, clays or sandy layers are interbedded between shales or sandstones. It is often found that a slope fails with large sections of slip surface along one particular bed (e.g., clays or sandy layers), which can also be seen as weak horizons within sedimentary dip slopes. The presence of weak horizons within slopes plays a significant role in the failure and kinematics of slopes (Wang et al., 2010; Geertsema et al., 2006; Bromhead and Ibsen, 2004; Pinyol et al., 2012; Liu and Koyi, 2013b). As such, it is important to understand the effect of weak horizons on both the failure mechanism of slopes and the kinematics and internal deformation of the failure mass.

Some studies have attributed slope failure to the presence of a weak horizon within the slope. For example, Hancox (2008) presented that a weak clay layer was the underlying cause of the 1979 Abbotsford landslide. Xu et al. (2010) investigated the causes of a catastrophic rockslide-debris flow in Wulong, China, and found that the limestone blocks slid along a weak interlayer of shale and the rupture surface of the slide was seated within the weak interlayer. Deng et al. (2011) suggested that the main part of the sliding plane was a thin weak layer (weathered tuff sandy layer) in a slope failure at Yokowatashi, Ojiya induced by the 2004 Niigata-ken Chuetsu earthquake in Japan. Petley et al. (2002) analyzed the movement pattern of five landslides which occurred across existing weak planes, for example, Giau Pass landslide in Italy, Abbotsford landslide in New Zealand, Tessina landslide of Italy etc., and concluded that these landslides slid on a pre-existing shear surface rather than a shear surface generated by crack propagation.

Conventional studies on slope stability analysis have employed limit equilibrium methods to determine the critical failure surface for non-homogeneous slopes with a horizontal or inclined weak horizon, and concluded that the critical failure surface is contained within weak horizons of the slopes (Lam and Fredlund, 1993; Goh, 1999; Huang and Tsai, 2000; Bolton et al., 2003). Some other studies have focused on the role of weak horizons on slope failure using numerical (Griffiths and Lane, 1999; Wei et al., 2009; Liu and Koyi, 2013b) and physical modeling (Lourenco et al., 2006; Wang et al., 2010). These studies showed that a weak horizon governs the location of the slip surface within the slope, and may induce larger displacement compared with homogeneous slopes. Previous studies of the effect of weak horizons on slope stability have mainly focused on the failure modes of slopes, i.e., how the failure surfaces progress within slopes. However, very few studies focused on the effect of orientation, location, and dimension of a weak horizon on the slope stability and mass movement related to a slope failure.

1.3 Thesis objectives

The following problems of landslide dynamics are still not clear: the spatial and temporal changes of the mass movement in terms of displacement and velocity within the failure mass, the failure mass area (i.e., how much mass will move), the impact of mechanical parameters (i.e., internal friction angle and cohesive strength) of slope material on the kinematics and internal deformation of the failure mass, how a weak horizon affects the failure mass movement and so on. The general objective of this thesis is to investigate the flow-like mass movement by focusing on these problems using three different methods, i.e., numerical and physical modeling, and field studies of natural landslides.

Using numerical modeling, the aims of Paper I and Paper II are described as below.

(1) To investigate in detail the two dimensional granular mass movement by focusing on the spatial and temporal changes in kinematics and internal deformation parameters such as velocity vectors, displacement vectors, and strain.

(2) To study the effect of two main mechanical parameters, coefficient of internal friction and cohesive strength on the internal deformation of granular slopes by running a series of numerical homogeneous slope models.

(3) To study the effect of orientation, location, and dimension of a weak horizon on kinematics and internal deformation of the failure mass movement within an unstable slope by running a series of numerical slope models with a weak horizon.

Using physical modeling and field studies of natural landslides, the aims of Paper III and Paper IV are described as below.

(1) To investigate the three dimensional internal deformation of a granular failure mass during the collapse of granular slopes, by focusing on the internal deformation structures and their spatial and temporal distribution. To compare the results of physical models with detailed case studies to outline the mode of failure of unstable slopes.

(2) To study the effect of the properties of the basal runout surface (i.e., smooth or rough, rigid or deformable and different deformable materials) on the internal deformation structures, the runout distance and the final topography of the granular slope.

(3) To study how weak horizons influence the mode of internal deformation and the spatial and temporal distribution of the structures within the failure mass during the collapse of unstable granular slopes, the location of the failure surfaces, and displacement along the failure surfaces using a series of physical models.

2 Methodology

2.1 Discrete element method

Two-dimensional Particle Flow Code (PFC^{2D}), which is one type of discrete element method, was proposed to be a suitable tool to simulate the granular assemblies by Cundall and Strack (1979). A general PFC^{2D} model simulates the mechanical behavior of a system which consists of a collection of particles with different sizes. The particles are circular rigid bodies with a finite mass that can move independently from one another and can both translate and rotate (Potyondy and Cundall, 2004). The rigid particles, which interact only at soft contacts, are allowed to overlap one another, and all overlaps (i.e., a point) are small in relation to particle size. The particles can also be bonded together at contacts, and the bonds between them carry load and can break. The mechanical behavior of this system is described by the movement of each particle and the force and moment acting at each contact. Newton's laws of motion provide the fundamental relationship between relative particle motion and the resultant forces and moments causing that motion (Itasca Consulting Group Inc., 2008).

The mechanical behavior occurring at a contact is achieved through the use of contact models, which may consist of up to three parts: a contact stiffness model, a slip model, and a bonding model (Itasca Consulting Group Inc., 2008). (1) A contact stiffness model provides an elastic relation between the contact force and relative displacement. The contact stiffnesses relate the contact forces and relative displacements in the normal and shear directions. (2) A slip model enforces a relation between shear and normal force, such that two entities (for example, particles) in contact may slide relative to one another. The slip condition occurs when the shear component of force reaches the maximum allowable shear contact force, which is taken to be the minimum friction coefficient of the two entities in contact multiplied by the magnitude of the compressive normal component of force. (3) Two types of bonds, contact bonds and parallel bonds, can be introduced at particle-particle contacts. Contact bonds reproduce the effect of an adhesion acting over the contact point, whereas parallel bonds reproduce the effect of additional material (for example, cementation) acting over either a circular or rectangular cross section lying between particles. Both types of bonds provide the contacts with normal and shear bond strengths and break when their strengths are exceeded. However, the parallel bond also provides ce-

mentatious material existing between the two particles with stiffnesses, which describe the force-displacement behavior of the material. The cement-filled (parallel bond) contacts experience compressive, tensile, and shear loading and also may transmit a bending moment between the particles; however, the empty (contact bond) contacts experience only compressive and shear loading. In general, a contact bond model is the simplified form of a parallel bond model (Potyondy and Cundall, 2004). Parallel bonds are often used to simulate rock (for example, sandstone or granite) as a heterogeneous material comprised of cemented grains. As such, to simplify the models, we chose the contact bond model rather than the parallel bond model to simulate cohesive granular materials in this thesis.

A contact bond provides each contact point with a tensile normal contact bond strength and shear contact bond strength, which allows a tensile force to develop between two particles. If the magnitude of the tensile normal or shear contact force exceeds the respective strength, the bond breaks. It is worth to mention that the slip model is not active until a contact bond is broken. Meanwhile, the contact stiffness and slip models are used to simulate non-cohesive granular materials.

The calculation cycle in PFC^{2D} is a time-stepping algorithm that consists of the repeated application of the law of motion to each particle, a force-displacement law to each contact, and a constant updating of wall positions (Figure 2.1; Itasca Consulting Group Inc., 2008). At the start of each time-step, the set of contacts is updated from the known particle and wall positions. The force-displacement law is then applied to each contact to update the contact forces based on the relative motion between the two entities at the contact and the contact constitutive model. Secondly, the law of motion is applied to each particle to update its velocity and position based on the resultant force and moment arising from the contact forces and any body forces acting on the particle.

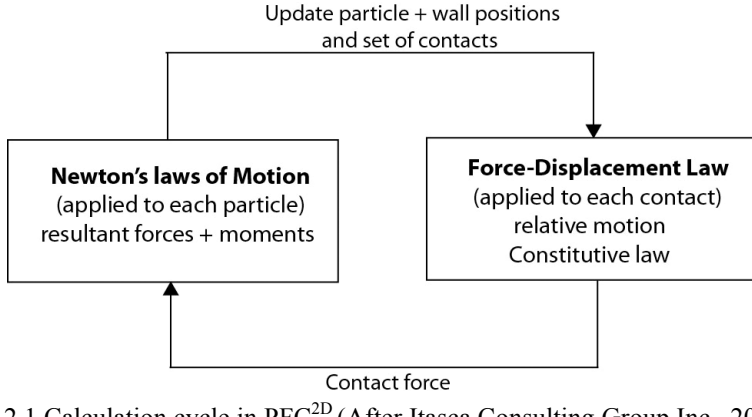

Figure 2.1 Calculation cycle in PFC^{2D} (After Itasca Consulting Group Inc., 2008)

In PFC^{2D}, the micro-mechanical properties for the particles are not coincident with macro-mechanical (bulk) properties of the target material. In other words, the input micro-properties in PFC^{2D} consist of the particle size distribution, particle stiffness, particle friction coefficient and bond strengths, whereas the macro-properties include elastic constants, internal friction angle and cohesive strength. To obtain the proper micro-properties for the particles in PFC^{2D}, numerical biaxial compressive tests and Brazilian tests are required to be performed before numerical simulation. By performing a series of numerical tests with different confining pressures, the Mohr-Coulomb failure envelope can be established, from which we can get the internal friction angle and cohesive strength for the simulated material in the numerical sample. The input micro-properties can be varied by trial-and-error until the macro-properties of the sample match the known macro-properties of the target material. Further information of choosing micro-properties by numerical experiments can be found in Cundall (1999), Wang et al. (2003), Imre (2004), Valentino et al. (2008), Itasca Consulting Group Inc. (2008), Cheng et al. (2009) and Tang et al. (2009).

PFC^{2D} has been widely adopted to simulate problems involving large deformation and fast movement generated by granular mass movement (Crosta et al., 2001; Wang et al., 2003; Imre, 2004; Valentino et al., 2008; Thompson et al., 2009; Tang et al., 2009; Thompson et al., 2010; Gabrieli et al., 2011; Li et al., 2012; Liu and Koyi, 2013a, b). These studies have demonstrated the capability of PFC^{2D} for investigating these types of problems.

2.2 Physical experiments

The numerical code (PFC^{2D}) that was used in this thesis could not simulate the particle size on a real scale, which causes the number of the particles to increase dramatically and requires far more computation time. It neither could simulate the three dimensional models. As such, physical experiments were performed to supplement the numerical method.

Koyi (1997) reviewed the development of analogue modeling to simulate and investigate the structures formed due to the deformation of rocks, and concluded that analogue modeling (i.e., sandbox modeling) has played an important role in the understanding of tectonic processes. Some researchers have been using sandbox models to investigate the gravitational deformation during slope instabilities triggered by fluid overpressure (Mourgues and Cobbold, 2006; Lacoste et al., 2011; Le Cossec et al., 2011). Mourgues and Cobbold (2006) emphasized that fluid overpressure facilitated propagation of the detachment and extensional deformation, and the angle of fault dip was affected by fluid pressure and frictional resistance at the base. Lacoste et al. (2011) found that in the case of a continued incision, normal faults propagated far upslope from the valley flanks; otherwise, the contractional slope

toe blocked further sliding. Le Cossec et al. (2011) showed that the fluid overpressure can trigger spontaneous dismemberment of a stable cliff, and the region of the model located near the initial cliff spread seaward and generated a series of normal faults that propagated landward, forming a frontal toe.

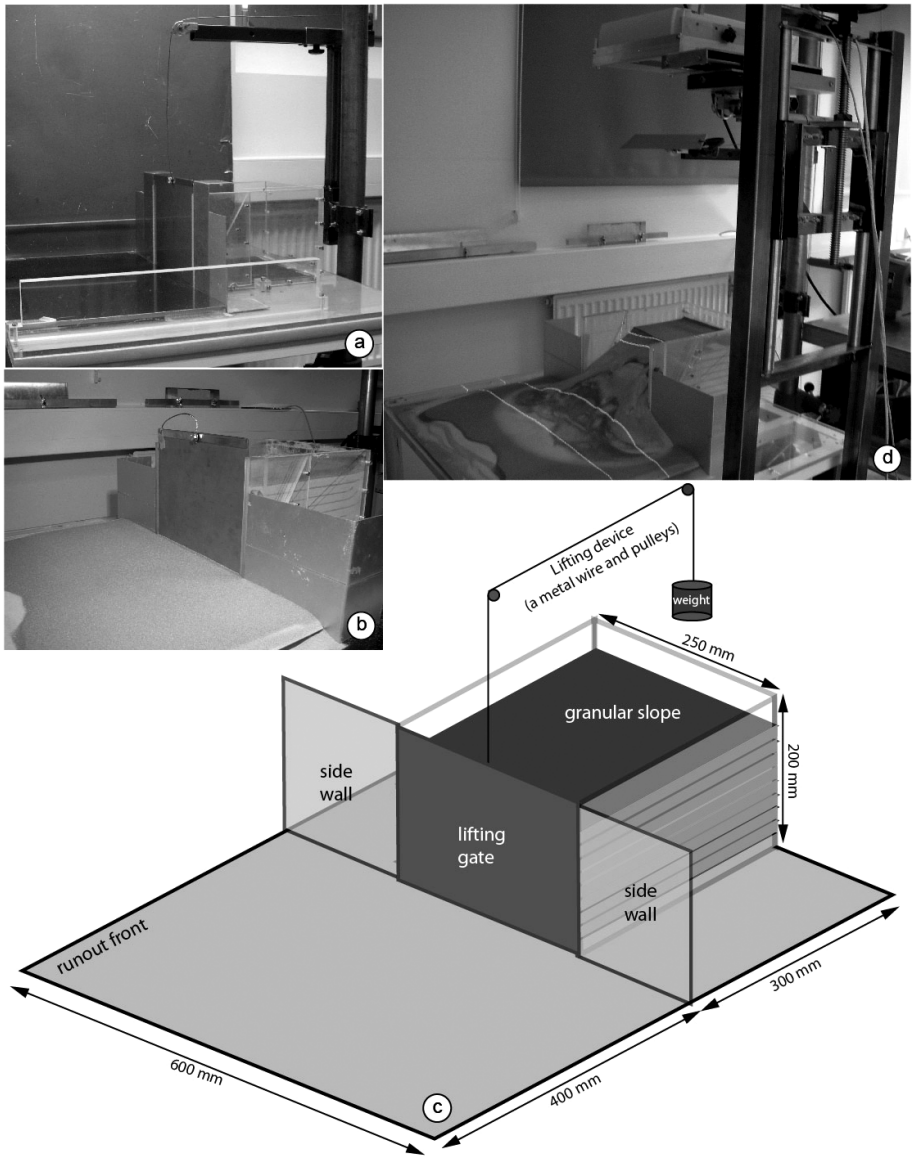

Figure 2.2 (a) Photo of the experiment device including the Perspex box, runout front part and lifting device (b) Photo of the physical model before deformation (c) Schematic drawing of the experiment device with the dimensions (d) Photo of the physical model after deformation and the high-resolution NextEngine 3D laser scanner.

In this thesis, sandbox models were used to investigate the collapse of unstable granular slopes. Experiments were carried out with two different granular materials: quartz sand of density 1.53 g/cm^3, grain size of 80-120 μm and internal friction angle of 33º; glass beads of density 1.46 g/cm^3, grain size of 50-100 μm and internal friction angle of 20º (Koyi and Vendeville, 2003; Maillot and Koyi, 2006; Liu et al., 2013). Quartz sand (relatively high friction) was used to simulate the granular slope, whereas glass beads (relatively low friction) was used to simulate the weak horizon embedded within the slope and/or runout base.

The in-house designed experimental device consists of two parts (Figure 2.2). One is a Perspex box (length 300 mm, width 250 mm, and height 200 mm) which has three fixed sides and a movable fourth side (i.e., a lifting gate) (Figure 2.2a). This lifting gate is a thin (1 mm thick) metal wall which can be pulled upwards, i.e., lifted at a high speed forming a free side. The box is filled with granular material to simulate an unstable slope (Figure 2.2b). The lifting gate keeps the granular material of the otherwise unstable slope in place. The surface of the gate is smooth, giving a friction coefficient of 0.23 with the sand mass which it keeps in place. The gate can be lifted up quickly and vertically by a lifting system made of a metal wire and pulleys once a weight is dropped (Figure 2.2c). The second part of the experimental setup is the runout front part which is 400 mm long and 600 mm wide. The area (i.e., both the width and the length) of the runout front surface is large enough to support a failure mass during the collapse of the granular slope. We scanned the slope surface before and after deformation by a high-resolution NextEngine 3D laser scanner (Figure 2.2d).

2.3 Natural landslides

The thesis investigated four natural failed slopes in Sweden, including landslide 1 along the Lärje River valley to the northeast of Göteborg, and landslides 2-4 along the Ångerman River near Sollefteå (Figure 2.3). In the Lärje River valley, quick clay dominates, and often attains a thickness of 50-60 meters (Magnusson, 1978). Only in the immediate vicinity of the river, some fluvial deposits (clay and silt) are found, while coarser material is rare. Along the Ångerman River, fine silt dominates, but coarse silt and sand are also found. The typical profile of Quaternary deposits along the Ångerman River consists of a top bed of coarse silt, sand and fine gravel, which is underlain by varved silt and clay (Lundqvist, 1987). The thesis mainly focused on the internal deformation structures by cutting cross-sections and scanning slope surfaces at/of some of the landslides. Through the topography of the failed slopes and/or internal structures within the failure mass, the kinematics and dynamics of these landslides were investigated.

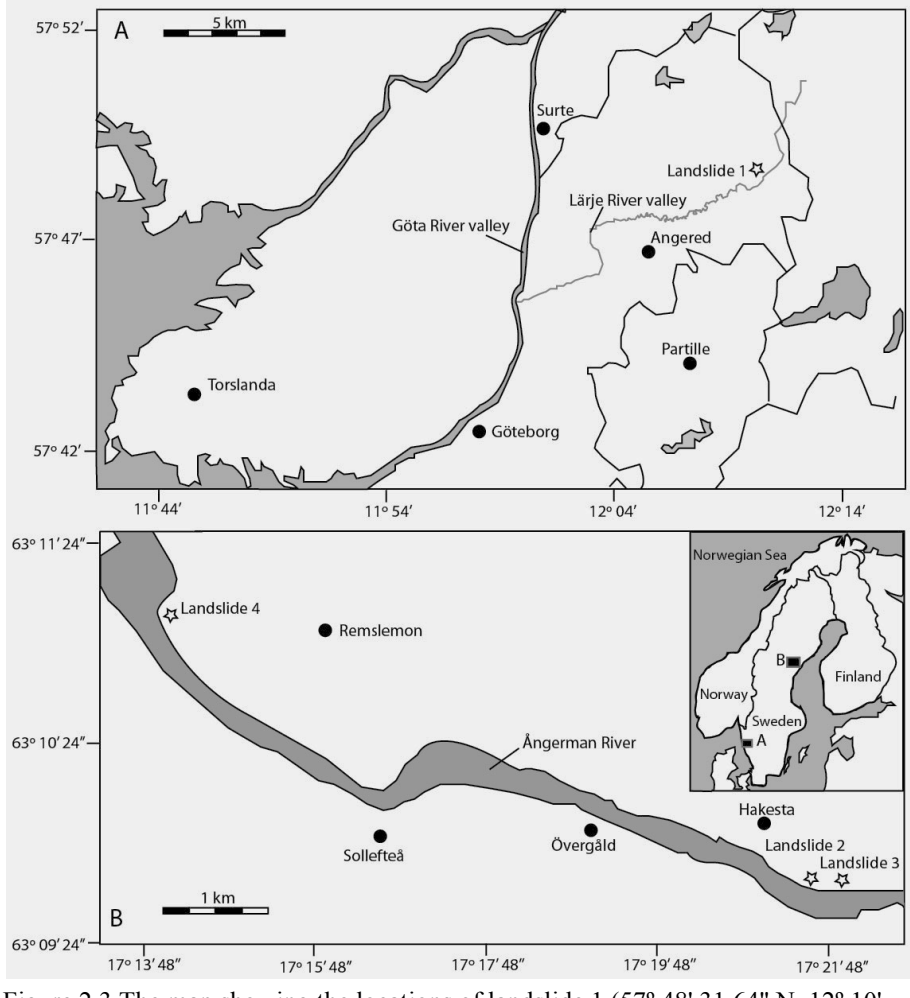

Figure 2.3 The map showing the locations of landslide 1 (57º 48' 31.64" N, 12º 10' 11.01" E) along the Lärje River valley to the northeast of Göteborg (A) and landslide 2 (63º 9' 41.88" N, 17º 21' 30.30" E), landslide 3 (63º 9' 40.50" N, 17º 21' 52.38" E), and landslide 4 (63º 11' 2.91" N, 17º 14' 7.78" E) along the Ångerman River near Sollefteå (B).

3 Summary of the papers

3.1 Kinematics and internal deformation of granular slopes: insights from discrete element modeling

Paper I monitored and quantified the kinematics and internal deformation of granular mass movement in two-dimensional geometry during the flow-like movement of a slope using the particle flow method. Two kinds of unstable granular slopes were investigated, non-cohesive and cohesive granular slopes. Three different internal friction angles and cohesive strengths were considered to systematically investigate their effect on the kinematics and internal deformation of the failure mass. The failure mass in each model displaced and deformed in the gravity field onto a flat basal ground surface to form a new topography. Model results show the following features related to a failure mass.

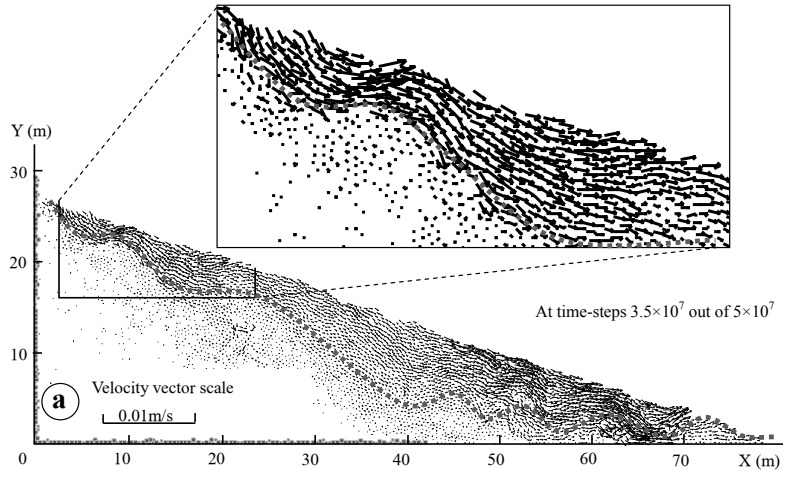

Figure 3.1 Velocity vector fields at one intermediate stages in a non-cohesive model with coefficient of internal friction μ=0.34. The length of the velocity vector represents the magnitude of velocity and the arrows describe the directions of velocity vectors at the location. The dashed line represents the orientation of velocity vectors at each location.

The failure mass flows downwards in an undulating pattern with a distinctive velocity heterogeneity (Figure 3.1). The undulating pattern, which occurs in all models, varies between different models. Coefficient of internal

friction and cohesion govern the pattern. Within the same model, the wavelength and the amplitude of the waves can vary both in space and time. The undulating pattern of movement is also shown in the displacement contour lines and the pattern of the distribution of extensional strain axes. However, model results show that, in the absence of a weak horizon, the shallow part of the slope moves faster and further than the deeper part of the slope.

The slope surface topography changes from a straight line to curved lines with slope breaks in a convex geometry, i.e., with the slope being steeper towards its toe during downward flowing of the mass. The non-cohesive models stabilize when the slope angle at the lower part decreases from the initial slope angle to approximate its internal friction angle (angle of repose), while the cohesive models stabilize with a slope angle larger than its internal friction angle due to the effect of cohesion.

The amount of the failure mass increases with time during the downslope movement, indicating that additional material is incorporated and start flowing during mass movement. In turn, this demonstrates that as the mass travels downslope, the position of the failure surface changes by incorporating material initially situated deeper during mass movement.

Dilatant grain shearing flow is a dominating mechanism in the movement of granular slopes. The granular mass dilates as it travels downslope. Porosity change is observed to be different between non-cohesive and cohesive models. In non-cohesive models, porosity increases significantly to a peak value and remains constant during the mass movement, whereas in cohesive models, porosity increases gradually to a peak, which is followed by a slight decrease of porosity. Cohesive models show that downslope movement of the mass results in bond breakage and formation of micro-cracks. The failure mass deforms internally in a heterogeneous way with the largest strain concentrating in the top (head) and bottom (toe) of the failure mass.

Kinematics and internal deformation of the failure mass are influenced significantly by the internal friction angles and cohesive strengths. The failure mass flows faster and further in the models with lower internal friction and cohesion. The runout distance of the final deposit is larger in the model with lower internal friction and cohesion. The amount of the failure mass increases as the internal friction and cohesion decreases, i.e., an inverse relationship. Dilatation within the failure mass (i.e., porosity) is proportional to both internal friction and cohesion; highest dilatation is seen in the model with largest internal friction and cohesion. Two-dimensional strain grows larger in the model with higher internal friction and cohesion.

3.2 The impact of a weak horizon on kinematics and internal deformation of a failure mass using discrete element method

Paper II investigated the effect of the presence and geometry (i.e., orientation, location and dimension) of a weak horizon on slope stability and the failure mass movement within an unstable slope using discrete element method.

Two kinds of cases with a weak horizon were studied, one unstable homogeneous slope with low shear strength (cohesive strength c=50 kPa, coefficient of internal friction μ=0.57) and two stable homogeneous slopes with high shear strength by increasing cohesive strength (c=60 kPa, μ=0.57) or increasing coefficient of internal friction (c=50 kPa, μ=0.7). In the three sets of slope models, there was a weak horizon with a finite thickness embedded within the slope. The weak horizon possessed much lower shear strength (c=0, μ=0.34) than that of the slope material in each model. In each set, two different thicknesses and locations for the weak horizons were considered to systematically investigate the effect of these parameters on the mass movement. In addition, the dip of the weak horizon was changed where in some models, it was parallel to the slope and in others it was dipping either steeper or gentler than the slope. We analyzed both kinematics and internal deformation of the failure mass in all models. Model results illustrate that in slope models with both high shear strength and low shear strength, a weak horizon strongly influences kinematics and internal deformation of the slope.

The presence of a weak horizon may increase or decrease displacement within the failure mass, depending on the orientation, location and dimension of the weak horizon within the slope. The thickness of the weak horizon has a positive impact on the amount of displacement of the failure mass; the thicker the weak horizon, the greater is the displacement. A weak horizon dipping steeper than the slope causes less displacement than a weak horizon dipping gentler than the slope surface. A weak horizon at a shallower location causes larger displacement of the failure mass; however, the location of a weak horizon does not affect the displacement as significantly as the thickness.

The failure surface and the amount of the failure mass are influenced directly by the orientation, location and dimension of the weak horizon. However, the presence of a weak horizon does not necessarily destabilize a slope under the condition of the slope with relatively high shear strength. For a cohesionless weak horizon with a small coefficient of internal friction (0.34), location (i.e., how deep the weak horizon is located within the slope), its dip relative to the slope and its dimension are three main factors which govern the stability of the slope and the failure mass movement.

Our model results also show that strain varies within the failure mass with the largest strain being located within the weak horizon with extensional axes parallel to its dip (Figure 3.2). However, in the homogeneous model, the largest strain is located near the slope surface.

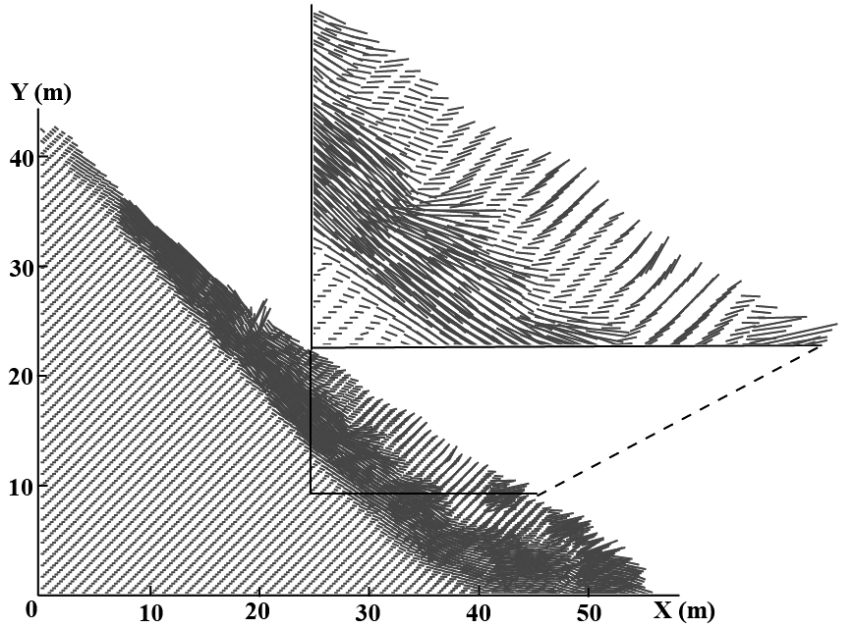

Figure 3.2 Distribution of extension infinitesimal axes in a model (c=50 kPa, μ=0.57) with a 2.6 m thick and shallow-located weak horizon parallel to the slope surface.

3.3 Kinematics and 3-D internal deformation of granular slopes: analogue models and natural landslides

Paper III investigated the kinematics and internal deformation during the collapse of an unstable granular slope, using results from a series of analogue models, and field observations, scanned data and sections of natural landslides. We have also studied the effect of friction and deformability of the runout base on internal deformation within a granular slope by performing a series of slope models with different runout bases (smooth or rough, rigid or deformable, and different deformable materials).

Model results show that a landslide consists of more than one single "pulse" of mass slide. The first pulse, which carries the largest mass downslope, is displaced furthest, forming the greatest spread of runout. In contrast, the later pulses are smaller in size and are displaced on top of the first pulse over a much smaller runout distance. The final surficial pulse shapes the slope surface. These results show that the failure mass of a granular slope collapses down along different-generation failure surfaces at different stages, instead of along only one failure surface. The failure surfaces of the failure mass change both spatially and temporally. Younger failure surfaces form in the back of the older ones by incorporating additional new material from the head of the slope. Dips of these failure surfaces decrease with time. As a result, the collapse of granular slopes results in different-generation extensional faults in the back of the slope, and contractional structures (overturned folds, sheath folds and thrusts) in the toe of the slope (Figure 3.3).

Model results also demonstrate that the friction and deformability of the runout base have a significant influence on the kinematics and internal deformation of a granular slope. In the case of a granular slope with a rigid runout base, displacement along the first-generation failure surface is larger in the model with lower basal friction. In contrast, the granular slope has largest displacement along the first-generation failure surface due to the erosion of the runout material in the back of the slope in the model with deformable runout base (glass beads). The runout distance increases with decreasing basal friction of a rigid runout base, but is the shortest in the model with deformable runout base. The topography in the lower part of the slope is much gentler in the model with lower friction rigid runout base. The volume of the failure mass decreases with increasing basal friction of the rigid runout base. More extensional faults occur in the model with lower basal friction, whereas more shortening structures form in the model with higher basal friction.

Model results are compared with natural landslides where local profiles were dug in order to decipher the internal structures of the failure mass. Good agreements between the analogue models and the natural landslides are found for the collapse of a granular slope. As in the models, our field

observations also indicate the presence of at least two generations of such failure surfaces, where the older ones are steeper and cut by the shallow-dipping younger ones (Figure 3.4).

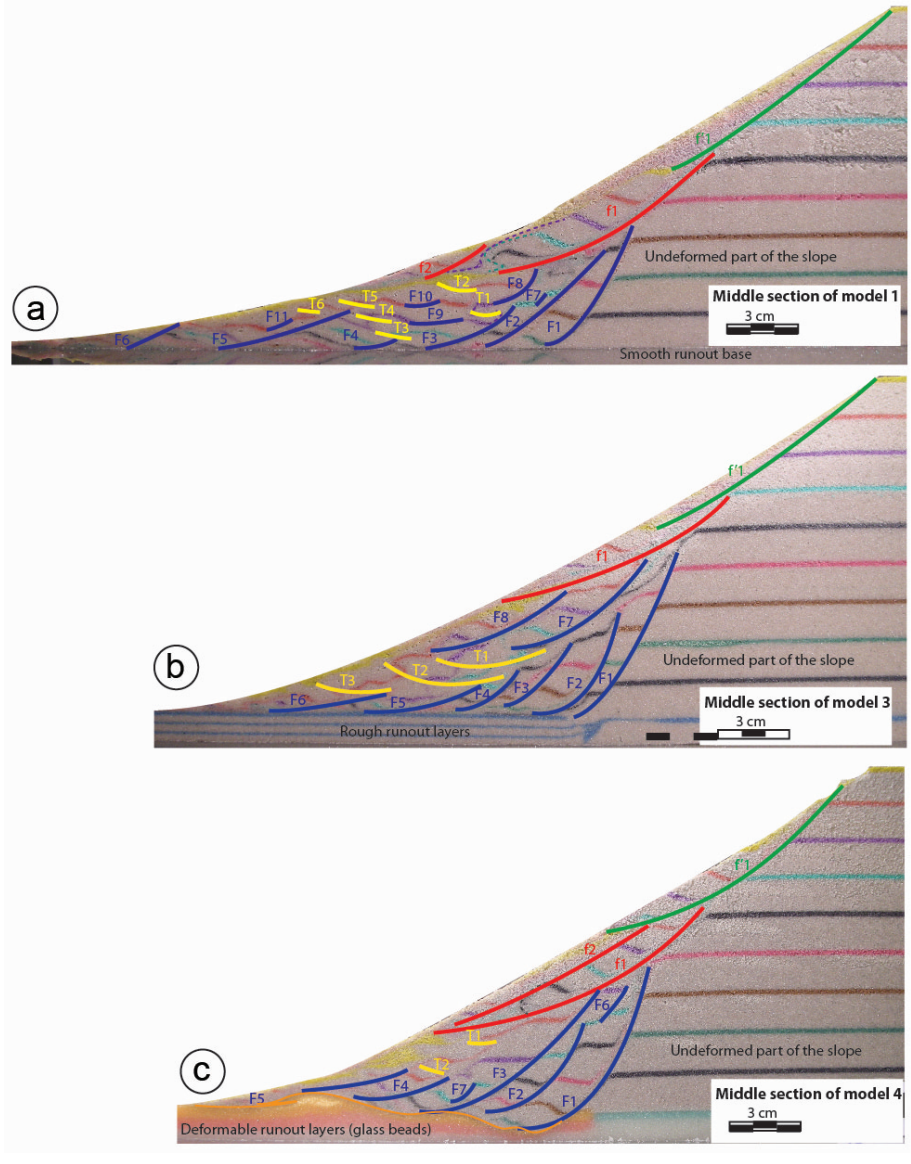

Figure 3.3 Internal deformation structures within the middle section along the dip direction in models with smooth (a), rough (b), or deformable bases (c). Blue, red and green lines represent first, second and third generation extensional faults, respectively, whereas yellow lines depict thrust faults.

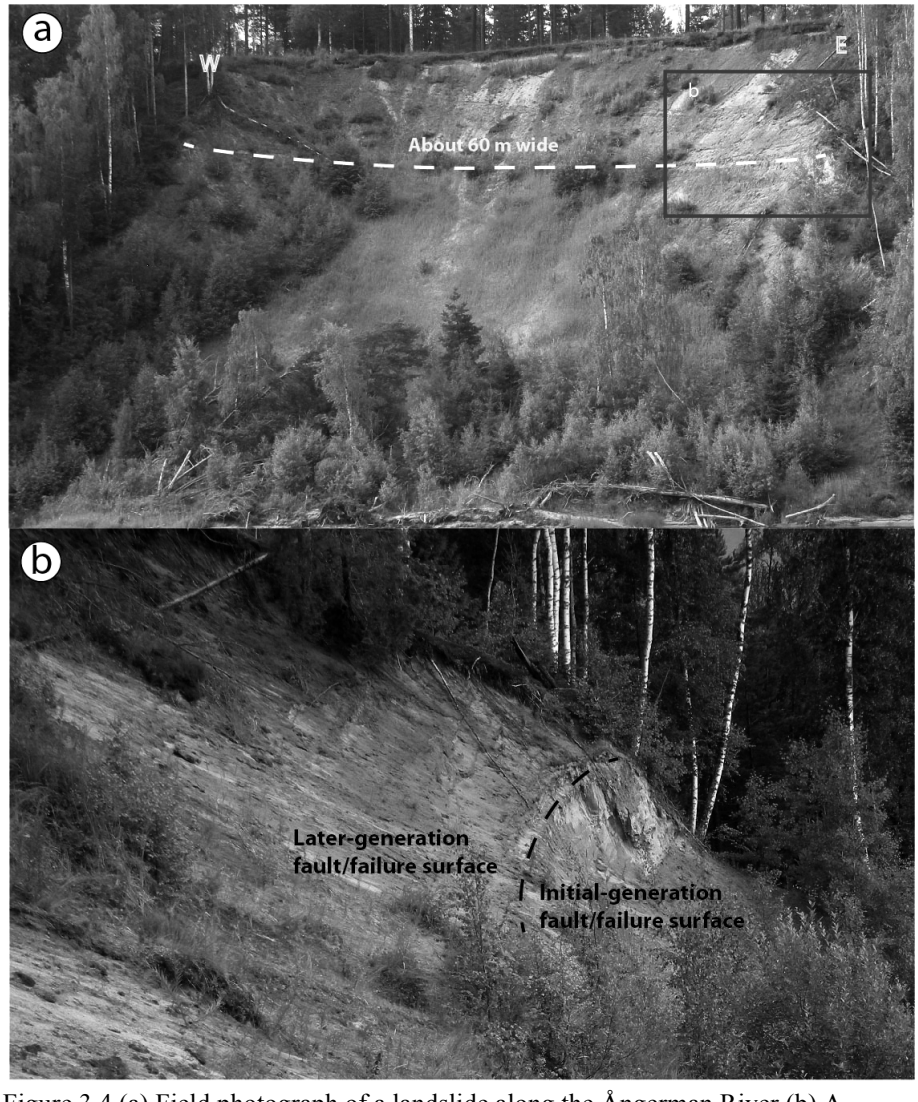

Figure 3.4 (a) Field photograph of a landslide along the Ångerman River (b) A closeup at the slope head showing two different-generation fault surfaces.

3.4 Analogue modeling of the collapse of non-homogeneous granular slopes along weak horizons

Paper IV investigated the effect of the orientation, location and thickness of a weak horizon on the stability/failure, kinematics and internal deformation of a granular slope using analogue modeling. The systematically designed analogue models simulate the collapse of non-homogeneous granular slopes by focusing on the spatial and temporal distribution of their internal deformation.

As shown in previous models, the granular slopes collapse in different pulses along different-generation failure surfaces. The first pulse carries the largest amount of the failure mass downslope, whereas the later pulses transports less amount of the failure mass. Each pulse deforms internally and has its own internal structures, resulting in formation of three or four generations of normal faults in the rear of the failure mass (Figure 3.5). First-generation normal faults are dipping steeply (about 60º), whereas later-generation normal faults are dipping gentler (about 40º). First-generation normal faults are seen in the lower part of the failure mass, cutting across the entire stratigraphy of the slope, and involve the bulk volume of the failure mass. In contrast, later-generation normal faults are seen in the upper part of the failure mass, do not penetrate deep in the failure mass, cut across the shallow units, and involve less amount of the failure mass. In addition, shortening structures generate in the front of the failure mass, where the shallow layers are folded or thrusted.

The initially horizontal passive layers rotate differently along different-generation normal faults within the failure mass. For each normal fault, dip of the passive layers increases with depth. Furthermore, layers rotate more along the gently-dipping normal faults in the toe of the slope (i.e., the later-generation normal faults) than the steeply-dipping normal faults in the rear of the slope (i.e., the first-generation normal faults).

The presence, orientation, location and thickness of a weak horizon have a significant influence on the failure mechanism and movement of granular slopes; it does not only change the dip and location of the different-generation failure surfaces, but also affect the displacement of the failure mass along the failure surfaces. The dip and stratigraphic location of the weak horizon dictate whether the weak horizon plays a role during the failure or not. The granular slope is more likely to fail along a weak horizon with a steeper dip. In addition, displacement along the first-generation failure zone/surface in the non-homogeneous models is larger than that in the homogeneous model, when the weak horizon is active during the initial collapse (i.e., the first-generation failure surface is located within the weak horizon). When the main failure surface is contained within a weak horizon, the dip and thickness of the weak horizon have a positive effect on the displacement of the failure mass, whereas a shallow-located weak horizon

causes larger displacement of the failure mass during the collapse of granular slopes. However, the final stable slope surface is not affected by the presence of the weak horizon within the slope; the final slope attains the angle of repose of the bulk granular material, i.e., about 30º.

Additionally, the internal structures within a failure mass are affected strongly by the presence of a weak horizon within the non-homogeneous granular slopes. The extensional faults differ in dip and amount of displacement they accommodate in the granular slopes containing a weak horizon with variable orientation, location or thickness. The distribution of shortening structures within the failure mass is also affected by the weak horizon. For instance, no shortening structures generate in the granular slopes with a weak horizon dipping 60º, where the weak horizon gets incorporated in the failure mass, providing a low friction horizon for the mass to glide on. In granular slopes with a weak horizon dipping 45º, shortening structures form in both the toe and the head of the failure mass; more shortening structures form in the model with a deeper-located weak horizon.

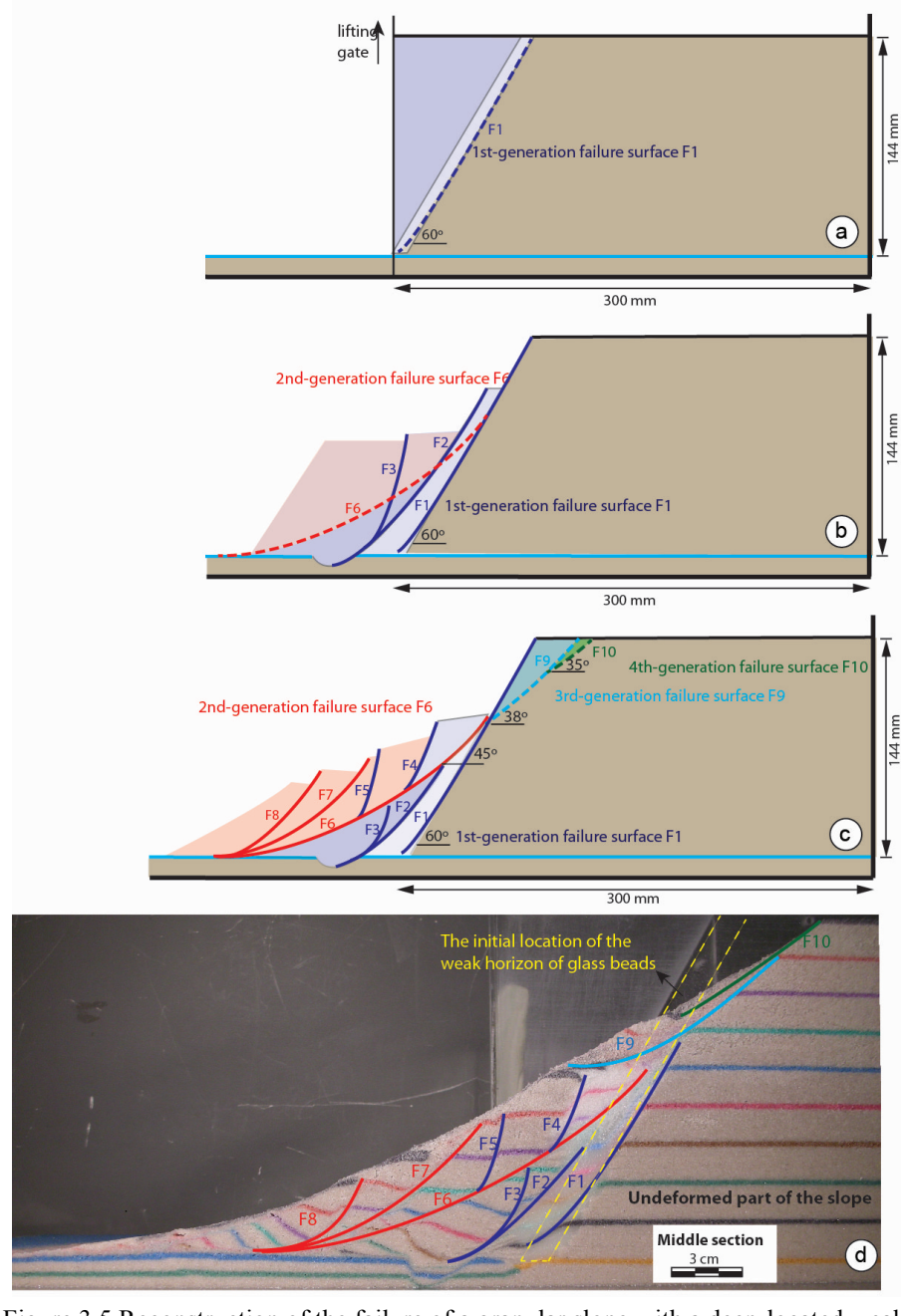

Figure 3.5 Reconstruction of the failure of a granular slope with a deep-located weak horizon dipping 60º, showing different-generation failure surfaces and internal structures within each pulse of the failure mass. Dark blue, red, light blue and green lines represent first, second, third and fourth generation extensional faults, respectively.

4 Conclusions

In this thesis, flow-like mass movement is investigated in response to gravity in granular slopes using discrete element modeling, analogue modeling, and field studies of natural landslides. Numerical models are used to monitor and quantify the spatial and temporal changes of velocity vectors, displacement vectors, and strain within a failure mass in both non-cohesive and cohesive granular slopes. Analogue models and natural landslides are used to decipher the three-dimensional internal deformation structures and their spatial and temporal distribution within a granular failure mass. We have also studied the effect of pre-existing weak horizons on the kinematics and internal deformation of granular slopes using both numerical and analogue modeling. The main findings are summarized as follows.

(1) Dilatant grain shearing flow is a dominating mechanism in the movement of granular slopes. The failure mass flows downwards in an undulating pattern with a distinctive velocity heterogeneity; displacement contours and the distribution of extensional strain also show this undulating pattern. The failure mass deforms internally in a heterogeneous way with the largest strain concentrating in the top (head) and bottom (toe) of the failure mass.

(2) The internal friction angle and cohesive strength strongly influence the kinematics and internal deformation of the failure mass. The mass flows faster and further in the models with lower internal friction and cohesion. The failure area is larger in models with lower internal friction and cohesion. Dilatation within the failure mass is proportional to both internal friction and cohesion; highest dilatation is seen in the model with largest internal friction and cohesion.

(3) The collapse of granular slopes results in different-generation extensional faults in the back of the slope, and contractional structures (overturned folds, sheath folds and thrusts) in the toe of the slope. The first-generation normal faults with a steep dip (about 60º) cut across the entire stratigraphy of the slope, whereas the later-generation normal faults with a gentle dip (about 40º) cut across the shallow units. Bedding rotates along these different generation faults; stratigraphically deeper beds rotate more than shallow ones. As in model results, our field observations indicate similar structural distribution within the failure mass and the presence of at least two generations of failure surfaces where the older ones are steeper and cut by the shallow-dipping younger ones.

(4) The friction and deformability of the runout base have a significant influence on the kinematics and internal deformation of a granular slope. The runout distance increases with decreasing basal friction of a rigid runout base, but is the shortest in the model with deformable runout base. The topography in the lower part of the slope is much gentler in the model with lower friction rigid runout base. The volume of the failure mass decreases with increasing basal friction of the rigid runout base. More extensional faults occur in the model with lower basal friction, whereas more shortening structures form in the model with higher basal friction.

(5) The presence of a weak horizon within the granular slope has a significant influence on the granular mass movement. The dip and stratigraphic location of the weak horizon dictate whether the weak horizon plays a role during the failure or not. The granular slope is more likely to fail along a weak horizon with a steeper dip. Displacement of the failure mass along the main failure surface (the weak horizon) increases with the dip and thickness of the weak horizon, but decreases with the depth of the weak horizon from the slope surface.

(6) The distribution of the internal structures within the failure mass is affected significantly by the weak horizon. The extensional faults differ in dip and amount of displacement they accommodate in the granular slopes containing a weak horizon with variable orientation, location or thickness. The distribution of shortening structures within the failure mass is also affected by the weak horizon. For instance, no shortening structures generate in the granular slopes with a weak horizon dipping 60º. In granular slopes with a weak horizon dipping 45º, shortening structures form in both the toe and the head of the failure mass; more shortening structures form in the model with a deeper-located weak horizon.

5 Sammanfattning på svenska

Skred med en hög flytkomponent, lång rörelsesträcka, hög hastighet och en stor volym av kollapsad massa är de svåraste att förhindra. De orsakar stora skador på egendom och förlust av människoliv över hela världen varje år. Därför är det ytterst viktigt att förstå kinematiken och dynamiken hos flödesliknande massrörelser bestående av granulärt material.

I denna avhandling har kinematik och intern deformation av flödesliknande massrörelser i granulära sluttningar som ett svar på gravitationen undersökts. Tre olika metoder har använts, diskretelementmodellering, analog modellering samt fältstudier av naturliga skred. Numeriska modeller används för att följa och kvantifiera spatiala och tidsmässiga förändringar av hastighetsvektorer, förflyttningsvektorer samt strain hos kollapsade massor i såväl ickekohesiva som kohesiva granulära sluttningar. Analoga modeller och naturliga skred nyttjas för att utröna tredimensionella interna deformationsstrukturer och deras spatiala och tidsmässiga utbredning inom en granulär kollapsad massa. Vi har också studerat effekten av två viktiga fysikaliska parametrar (den interna friktionskoefficienten och den sammanhållande kraften) på kinematiken och intern deformation av granulära sluttningar. Hänsyn har också tagits till karaktären av basytan över vilket skredet ”flyter” samt redan existerande svaga horisonter i skreden.

(1) Utvidgande skjuvningsflöden av partiklar är en dominerande mekanism i rörelsen hos granulära sluttningar. Den kollapsade massan flyter nedåt i ett undulerande mönster med tydliga hastighetsvariationer. Konturer som visar förflyttningen och utbredningen av strain på grund av töjning uppvisar även detta undulerande mönster. Inom samma modell kan såväl våglängden som vågornas amplitud variera både i rum och tid. Den kollapsade massan deformeras internt på ett heterogent vis med störst strain koncentrerat högst upp och längst ned.

(2) Den interna friktionsvinkeln och kohesionsstyrkan påverkar kraftigt kinematiken och den interna deformationen av den kollapsade massan. Det undulerande mönstret av hastighetsvektorer varierar mellan olika modeller vilket styrs av den interna friktionskoefficienten och kohesionen. Den kollapsade massan flyter snabbare och längre i modeller med lägre intern friktion och kohesion. Mängden av kollapsad massa ökar när den interna friktionen och kohesionen minskar, det vill säga de är omvänt proportionella gentemot varandra. Uttänjning i den kollapsade massan som visar sig genom porositet är proportionell till såväl intern friktion som kohesion; störst ut-

tänjning ses i den modell som har den största interna friktionen och kohesionen. Tvådimensionell strain växer mera i en modell med högre intern friktion och kohesion.

(3) Granulära sluttningar kollapsar i flera pulser. Den första pulsen, som för med sig den största massan neråt flyttar sig också längst. Den ger den största spridningen av utflödet. Däremot är de senare pulserna mindre och rör sig på toppen av den första pulsen över en betydligt kortare sträcka. Den sista ytliga pulsen skapar sluttningens yta. Kollaps av granulära sluttningar ger flera generationers förkastningar på grund av tänjning i den övre ändan av sluttningen. Sammanpressningsstrukturer som överstjälpta veck och överskjutningar påträffas vid sluttningens fot. Första generationens normalförkastningar med en brant stupning (omkring 60°) skär igenom sluttningens hela stratigrafi. Senare generationers normalförkastningar med en mer moderat stupning (omkring 40°) enbart skär igenom ytliga lager. De kollapsade ytorna och volymen av den kollapsade massan var föränderlig, både spatialt och tidsmässigt. Yngre ytor bildades längst upp på de äldre genom att de tog med sig nytt material från sluttningens översta del. Modellresultat jämförs med naturliga skred där profiler grävdes för att studera interna strukturer hos den kollapsade massan. Överensstämmelsen mellan analoga modeller och det som sker i samband med naturliga skred är god vad det gäller kollapsen av en sluttning som består av granulärt material.

(4) Friktion och deformation hos basytan där skredet flyter ut har en betydande påverkan på kinematik och intern deformation av en granulär sluttning. Flödesdistansen ökar med minskande friktion hos basytan förutsatt att denna är fast och rigid. Om ytan däremot är deformerbar blir flödesdistansen som kortast. Topografin i den lägre delen av sluttningen är ganska jämn i modellen med en rigid utflödesbasyta och låg friktion. Volymen av skredmassan minskar med ökad friktion mot den fasta rigida basytan. Fler förkastningar på grund av uttöjning finns i modellen med lägre basfriktion, medan sammanpressningsstrukturer bildas i modellen med högre basfriktion.

(5) Förekomsten av en svag horisont inne i en granulär sluttning har en betydande inverkan på den granulära massrörelsen. Stupningen och det stratigrafiska läget av den svaga horisonten bestämmer vilken roll den har under kollapsen. Det är större risk att en sluttning i granulärt material kollapsar om den svaga horisonten har brant stupning. Omflyttningen av skredmassan längs den svaga horisonten ökar med stupningen och tjockleken av denna horisont, men minskar med djupet av horisonten sett från sluttningens yta.

(6) Fördelningen av de interna strukturerna inom den kollapsade massan påverkas tydligt av den svaga horisonten. Förkastningar på grund av uttöjning varierar i stupning och rörelsemängd i granulära sluttningar som innehåller en svag horisont med olika riktningar, placering eller tjocklek. Fördelningen av sammanpressningsstrukturer inom den kollapsade massan påverkas också av den svaga horisonten. Till exempel uppstår inga sammanpressningsstrukturer i en granulär sluttning om den svaga horisonten stupar 60°. I

granulära sluttningar med en svag horisont som stupar 45° bildas kompressionsstrukturer både vid foten och toppen av den kollapsade massan. Flest sådana strukturer bildas i en modell med en djupare liggande svag horisont.

Acknowledgments

This study is financed by partly a PhD scholarship from Uppsala University and partly by Swedish Research Council (VR) through Hemin A. Koyi.

I would like to firstly express my deep gratitude to my main supervisor Prof. Hemin Koyi. I am grateful for being given the opportunity to work on this project in Uppsala University. Hemin brought me into the field of slope tectonics and helped me link deformation and features within landslides to structural geology and tectonic features. I appreciate his encouragement, guidance and support in my research during the past four years. I thank him for fruitful discussions about each manuscript. I also want to thank Hemin for introducing me to the field of analogue modeling. I would like to thank my co-supervisors, Dr. Jan Swantesson from Karlstad University and Dr. Faramarz Nilfouroushan for helping me doing the field work every summer. Thank all of them for being kind and friendly to me.

I would like to thank two people from the Geological Survey of Sweden (SGU), Mats Engdahl for showing us several landslides in Göteborg and Nils Dahlberg for providing us with a map showing the locations of landslides in Sollefteå. I thank Åke Wallmark for kindly helping us crossing the river in his boat to visit one landslide in Sollefteå.

I appreciate the help and friendship from the colleagues at our department. Thanks to Abigail Barker, Steffi Burchardt, Michael Krumbholz, Frances Deegan, Lara Blythe, Peter Dahlin, Ester M. Jolis, Kirsten Pedroza, Börje Dahren, Lukas Fuchs, David Budd, Iwona Klonowska, Peter Lazor, Håkan Sjöström, Karin Högdahl, Jochen Kamm, Arnaud Pharasyn, María García, Michael Schieschke, Juliane Hübert. The technical and administration staff at Geocenter are greatly appreciated for their work: Taher Mazloomian, Anna Callerholm, Tomas Nord, Ingegerd Ohlsson, Siv Petterson, Jeanette Flygare, Susanne Paul, Fatima Ryttare-Okorie, Zara Witt-Strömer. A special thanks to Ester and Börje: it was a pleasure to be your officemate! Thank you so much Jan Swantesson and Örjan Amcoff for translating my summary into Swedish.

Thanks to Chinese colleagues and friends in Uppsala University for their help and the good times we spent together: Hongling Deng, Chunling Shan, Dongjing Fu, Ping Yan, Fengjiao Zhang, Can Yang, Peng Yi, Peng He, Haizhou Wang, Biao Wang, Zhibing Yang, Shang Peng, Fei Huang.

Thanks to Lanru Jing and his wife Wenli Long for inviting me to their home for Chinese festivals during my stay in Sweden. Thank you to my

friends in Stockholm: Fuguo Tong, Bo Li, Mingzhi Liao, Liangchao Zou, Lin Ni for their friendship.

Finally, I would like to thank my parents and two sisters in China for their endless love and support. The biggest thanks goes to my husband Zhihong Zhao for his encouragement, support and love, and to my daughter Pengyan Zhao for being the best gift I've ever received in my life.

References

Barlar G., Antolini F., Barla M., Mensi E. and Piovano G. (2010) Monitoring of the Beauregard landslide (Aosta Valley, Italy) using advanced and conventional techniques. Engineering Geology 116, 218-235.

Bois T., Bouissou S. and Jaboyedoff M. (2012) Influence of structural heterogeneities and of large scale topography on imbricate gravitational rock slope failures: New insights from 3-D physical modeling and geomorphological analysis. Tectonophysics 526-529, 147-156.

Bolton H.P.J., Heymann G., and Groenwold A.A. (2003) Global search for critical failure surface in slope stability analysis. Engineering Optimization 35(1), 51-65.

Bromhead E.N. (2000) The stability of slopes. Taylor and Francis Group, New York.

Bromhead E.N. and Ibsen M.L. (2004) Bedding-controlled coastal landslides in Southeast Britain between Axmouth and the Thames Estuary. Landslides 1, 131-141.

Bui H.H., Fukagawa R., Sako K. and Ohno S. (2008) Lagrangian meshfree particles method (SPH) for large deformation and failure flows of geomaterial using elastic-plastic soil constitutive model. International Journal for Numerical and Analytical Methods in Geomechnics 32, 1537-1570.

Campbell C.S., Cleary P.W. and Hopkins M. (1995) Large-scale landslide simulations: global deformation, velocities and basal friction. Journal of Geophysical Research 100(85), 8267-8283.

Chen R.H., Kuo K.J., Chen Y.N. and Ku C.W. (2011) Model tests for studying the failure mechanism of dry granular soil slopes. Engineering Geology 119, 51-63.

Cheng Y.M., Liu Z.N., Song W.D. and Au S.K. (2009) Laboratory test and Particle Flow Simulation of silos problem with nonhomogeneous materials. Journal of Geotechnical and Geoenvironmental Engineering 135(11), 1754-1761.

Crosta G., Calvetti F., Imposimato S., Roddeman D., Frattini P. and Agliardi F. (2001) Granular flows and numerical modelling of landslides. Report of Damocles Project EVG1-CT-1999-00007.

Cundall P.A. (1999) Numerical experiments on rough joints in shear using a bonded particle model. Lecture Notes in Earth Sciences, Springer-Verlag, Berlin.

Cundall P.A. and Strack O.D.L. (1979) A discrete numerical model for granular assemblies. Geotechnique 29(1), 47-65.

Deng J., Kameya H., Miyashita Y., Kuwano J., Kuwano R. and Koseki J. (2011) Study on a failed dip slope with a thin sandy layer in 2004 Niigata-ken Chuetsu Earthquake. Engineering Geology 123, 302-314.

Gabrieli F., Lambert P., Cola S. and Calvetti F. (2011) Micromechanical modelling of erosion due to evaporation in a partially wet granular slope. International Journal for Numerical and Analytical Methods in Geomechanics, DOI: 10.1002/nag.1038.

Geertsema M., Clague J.J., Schwab J.W. and Evans S.G. (2006) An overview of recent large catastrophic landslides in northern British Columbia, Canada. Engineering Geology 83, 120-143.

Gili J.A., Corominas J. and Rius J. (2000) Using Global Positioning System techniques in landslide monitoring. Engineering Geology 55, 167-192.
Griffiths D.V. and Lane P.A. (1999) Slope stability analysis by finite elements. Geotechnique 49(3), 387-403.
Goh A.T.C. (1999) Genetic algorithm search for critical slip surface in multiple-wedge stability analysis. Canadian Geotechnical Journal 36 (2), 382-391.
Hancox G.T. (2008) The 1979 Abbotsford Landslide, Dunedin, New Zealand: a retrospective look at its nature and causes. Landslides 5, 177-188.
Hansen D. (1997) The angle of reach as a mobility index for small and large landslides. Canadian Geotechnical Journal 33, 1027-1029.
Huang C., and Tsai C. (2000) New method for 3D and asymmetrical slope stability analysis. Journal of Geotechnical and Geoenvironmental Engineering 126 (10), 917-927.
Hungr O. (1995) A model for the runout analysis of rapid flow slides, debris flows, and avalanches. Canadian Geotechnical Journal 32(4), 610-623.
Hungr O., Evans S.G., Bovis M.J., Hutchinson J.N. (2001) A review of the classification of landslides of flow type. Environmental and Engineering Geoscience. 7(3), 1-18.
Hungr O. (2003) Flow slides and flows in granular soils. In: Proceedings of International Workshop on Occurrence and Mechanisms of Flows In Natural Slopes and Earth Fills.
Hungr, O. (2008) Simplified models of spreading flow of dry granular material. Canadian Geotechnical Journal 45, 1156-1168.
Hungr O. (2009) Numerical modelling of the motion of rapid, flow-like landslides for hazard assessment. Journal of Civil Engeering 13(4), 281-287.
Hutchinson J.N. (1988) General Report: morphological and geotechnical parameters of landslides in relation to geology and hydrogeology In Bonnard C. (Editor), Proceedings, Fifth International Symposium on Landslides, A A Balkema, Rotterdam, Vol 1, pp 3-36.
Hutchinson J.N. (2004) Review of flow-like mass movements in granular and fine-grained materials. In: Picarelli L. (Editor), Proceedings, International.Workshop Occurrence and Mechanisms of Flows in Natural Slopes and Earthfills. Sorrento, Patron, Bologna, 3-16.
Imre B. (2004) Numerical slope stability simulations of the northern wall of eastern Candor Chasma (Mars) utilizing a distinct element method. Planetary and Space Science 52, 1303-1319.
Itasca Consulting Group Inc. (2008) PFC2D Particle Flow Code in 2 Dimensions User's Guide.
Koyi H. (1997) Analogue modeling: from a qualitative to a quantitative technique-a historical outline. Journal of Petroleum Geology, 20 (2), 223-238.
Koyi A.H., Vendeville B.C. (2003) The effect of decollement dip on geometry and kinematics of model accretionary wedges. Journal of Structural Geology 25, 1445-1450.
Lacoste A., Vendeville B.C., Loncke L. (2011) Influence of combined incision and fluid overpressure on slope stability: Experimental modelling and natural applications. Journal of Structural Geology 33, 731-742.
Lajeunesse E., Monnier J.B., Homsy G.M. (2005) Granular slumping on a horizontal surface. Physics of Fluids 17, 103302, DOI: 10.1063/1.2087687.
Lam L., and Fredlund D.G. (1993) A general limit equilibrium model for three-dimensional slope stability analysis. Canadian Geotechnical Journal 30, 905-919.

Le Cossec J., Duperret A., Vendeville B.C., Taibi S. (2011) Numerical and physical modelling of coastal cliff retreat processes between La Hève and Antifer capes, Normandy (NW France). Tectonophysics 510, 104-123.
Leong E.C. and Rahardjo H. (2012) Two and three-dimensional slope stability reanalyses of Bukit Batok slope. Computers and Geotechnics 42, 81-88.
Li W.C., Li H.J., Dai F.C. AND Lee L.M. (2012) Discrete element modeling of a rainfall-induced flowslide. Engineering Geology 149-150, 22-34.
Liu P., Li Z., Hoey T., Kincal C., Zhang J., Zeng Q. and Muller J.P. (2011) Using advanced InSAR time series techniques to monitor landslide movements in Badong of the Three Gorges region, China. Internal Journal of Applied Earth Observation and Geoinformation, DOI: 10.1016/j.jag.2011.10.010.
Liu Z., and Koyi H.A. (2013a) Kinematics and internal deformation of granular slopes: insights form discrete element modeling. Landslides, 10, 139-160.
Liu Z., and Koyi H.A. (2013b) The impact of a weak horizon on kinematics and internal deformation of a failure mass using discrete element modeling. Tectonophysics, 586, 95-111.
Liu Z., Koyi H.A., Swantesson J.O.H., Nifouroushan F. and Reshetyuk Y. (2013) Kinematics and 3-D internal deformation of granular slopes: Analogue models and natural landslides. Journal of Structural Geology, 53, 27-42.
Lourenco S.D.N., Sassa K., and Fukuoka H. (2006) Failure process and hydrologic response of a two layer physical model: Implications for rainfall-induced landslides. Geomorphology 73, 115-130.
Lube G., Huppert H.E., Sparks R.S.J., Freundt A. (2005) Collapses of two-dimensional granular columns. Physical Review E 72, 041301, DOI: 10.1103/PhysRevE.72.041301.
Lube G., Huppert H.E., Sparks R.S.J., Freundt A. (2007) Static and flowing regions in granular collapses down channels. Physics of Fluids 19, 043301, DOI: 10.1063/1.2712431.
Lundqvist J. (1987) Beskrivning till jordarskarta över Västernorrlands län och förutvarande Fjällsjö k: n. Sveriges Geologiska Undersökning. Ser. Ca 55.
Magnusson E. (1978) Beskrivning till jordartskartan Göteborg SO. Sveriges Geologiska Undersökning. Ser. Ae 26.
Maillot B., Koyi H. (2006) Thrust dip and thrust refraction in fault-bend folds: analogue models and theoretical predictions. Journal of Structural Geology 28, 36-49.
Miao T., Liu Z., Niu Y., Ma C. (2001) A sliding block model for the runout prediction of high-speed landslides. Canadian Geotechnical Journal 38(2), 217-226.
Mora P., Baldi P., Casula G., Fabris M., Ghirotti M., Mazzini E. and Pesci A. (2003) Global Positioning Systems and digital photogrammetry for the monitoring of mass movements: application to the Ca'di Malta landslide. Engineering Geology 38, 103-121.
Mourgues R., Cobbold P.R. (2006) Sandbox experiments on gravitational spreading and gliding in the presence of fluid overpressures. Journal of Structural Geology 28, 887-901.
Naghadehi M.Z., Jimenez R., KhaloKaKaie R. and Jalali S.M.E. (2011) A probabilistic systems methodology to analyze the importance of factors affecting the stability of rock slopes. Engineering Geology 118, 82-92.
Oppikofer T., Jaboyedoff M., Blikra L., Derron M.H. and Metzger R. (2009) Characterization and monitoring of the Åknes rockslide using terrestrial laser scanning. Natural Hazards and Earth System Sciences 9, 1003-1019.
Petley D.V., Bulmer M.H. and Murphy W. (2002) Patterns of movement in rotational and translational landslides. Geology 8, 719-722.

Peyret M., Djamour Y., Rizza M., Ritz J.F., Hurtrez J.E., Goudarzi M.A., Nankali H., Chery J., Dortz K.L. and Uri F. (2008). Monitoring of the large slow Kahrod landslide in Alborz mountain range (Iran) by GPS and SAR interferometry. Engineering Geology 100, 131-141.

Picarelli L., Olivares L., Comegna L. and Damiano E. (2008) Mechanical Aspects of Flow-like movements in granular and fine grained soils. Rock Mechanics and Rock Engineering 41 (1), 179-197.

Pinyol N.M., Alonso E.E., Corominas J., and Moya J. (2012) Canelles landslide: modelling rapid drawdown and fast potential sliding. Landslides 9, 33-51.

Potyondy D.O. and Cundall P.A. (2004) A bonded-particle model for rock. International Journal of Rock Mechanics and Mining Sciences 41, 1329-1364.

Roy S. and Mandal N. (2009) Modes of hill-slope failure under overburden loads: insights from physical and numerical models. Tectonophysics 473, 324-340.

Saintot A., Henderson I.H.C. and Derron M.H. (2011) Inheritance of ductile and brittle structures in the development of large rock slope instabilities: examples from western Norway. In: Jaboyedoff, M. (Ed.), Slope Tectonics, Geological Society, London, Special Publication 351, 27-78.

Siavoshi S., Kudrolli A. (2005) Failure of a granular step. Physical Review E 71, 051302, DOI: 10.1103/PhysRevE.71.051302.

Sturzenegger M. and Stead D. (2009) Quantifying discontinuity orientation and persistence on high mountain rock slopes and large landslides using terrestrial remote sensing techniques. Natural Hazards and Earth System Sciences 9, 267-287.

Tang C., Hu J., Lin M., Angelier J., Lu C., Chan Y. and Chu H. (2009) The Tsaoling landslide triggered by the Chi-Chi earthquake, Taiwan: Insights from a discrete element simulation. Engineering Geology 106, 1-19.

Teza G., Galgaro A., Zaltron N. and Genevois R. (2007) Terrestrial laser scanner to detect landslide displacement fields: a new approach. Internal Journal of Remote Sensing 28, 3425-3446.

Teza G., Pesci A., Genevois R. and Galgaro A. (2008) Characterization of landslide ground surface kinematics from terrestrial laser scanning and strain field computation. Geomorphology 97, 424-437.

Thompson N., Bennett M.R. and Petford N. (2009) Analyses on granular mass movement mechanics and deformation with distinct element numerical modeling: implications for large-scale rock and debris avalanches. Acta Geotechnica 4, 233-247.

Thompson N., Bennett M.R. and Petford N. (2010) Development of characteristic volcanic debris avalanche deposit structures: new insight from distinct element simulations. Journal of Volcanology and Geothermal Research 192, 191-200.

Valentino R., Barla G. and Montrasio L. (2008) Experimental analysis and micromechanical modelling of dry granular flow and impacts in laboratory flume tests. Rock Mechanics and Rock Engineering 41(1), 153-177.

Varnes D.J. (1978) Slope movement types and processes. In Schuster R.L. and Krizek R.J. (Editors), Landslides, Analysis and Control, Special report 176: Transportation Research Board, National Academy of Sciences, Washington, DC, pp 11-33.

Wang C., Tannant D.D. and Lilly P.A. (2003) Numerical analysis of the stability of heavily jointed rock slopes using PFC2D. International Journal of Rock Mechanics and Ming Sciences 40, 415-424.

Wang R., Zhang G. and Zhang J. (2010) Centrifuge modeling of clay slope with montmorillonite weak layer under rainfall conditions. Applied Clay Science 50, 386-394.

Wei W.B., Cheng Y.M. and Li L. (2009) Three-dimensional slope failure analysis by the strength reduction and limit equilibrium methods. Computers and Geotechnics 36, 70-80.
Xu Q., Fan X., Huang R., Yin Y., Hou S., Dong X. and Tang M. (2010) A catastrophic rockslide-debris flow in Wulong, Chongqing, China in 2009: background, characterization and causes. Landslides 7, 75-87.

Acta Universitatis Upsaliensis

Digital Comprehensive Summaries of Uppsala Dissertations from the Faculty of Science and Technology 1153

Editor: The Dean of the Faculty of Science and Technology

A doctoral dissertation from the Faculty of Science and Technology, Uppsala University, is usually a summary of a number of papers. A few copies of the complete dissertation are kept at major Swedish research libraries, while the summary alone is distributed internationally through the series Digital Comprehensive Summaries of Uppsala Dissertations from the Faculty of Science and Technology. (Prior to January, 2005, the series was published under the title "Comprehensive Summaries of Uppsala Dissertations from the Faculty of Science and Technology".)

Distribution: publications.uu.se
urn:nbn:se:uu:diva-223792

ACTA
UNIVERSITATIS
UPSALIENSIS
UPPSALA
2014